Neurology®
The most widely read and highly cited peer-reviewed neurology journal
The Official Journal of the American Academy of Neurology

AMERICAN ACADEMY OF NEUROLOGY®

Neurology Publish Ahead of Print
DOI: 10.1212/WNL.0000000000200776

Longitudinal Changes in MRI Muscle Morphometry and Composition in People With Inclusion Body Myositis

Author(s):
Didier Laurent, PhD[1]; Jon Riek, PhD[2]; Christopher DJ Sinclair, PhD[3]; Parul Houston, PhD[1]; Ronenn Roubenoff, MD[1]; Dimitris A Papanicolaou, MD[1]; Attila Nagy, PhD[4, 5]; Steve Pieper, PhD[4]; Tarek A Yousry, MD[3, 6]; Michael G Hanna, MD, FRCP[7]; John S Thornton, PhD[3]; Pedro M Machado, MD, PhD[7, 8]

Corresponding Author:
Didier Laurent, didier.laurent@novartis.com

Affiliation Information for All Authors: 1. Novartis Institutes for Biomedical Research, Basel, Switzerland; 2. BioTel Research, Rochester, NY, USA; 3. Neuroradiological Academic Unit, UCL Institute of Neurology, London, UK; 4. Isomics Inc, Cambridge, MA, USA; 5. Department of Medical Physics and Informatics, University of Szeged, Hungary; 6. Lysholm Department of Neuroradiology, National Hospital for Neurology and Neurosurgery, London, UK; 7. Department of Neuromuscular Diseases, UCL Queen Square Institute of Neurology, University College London, London, UK; 8. Centre for Rheumatology, Department of Inflammation, Division of Medicine, University College London, London, UK

Equal Author Contribution:
Didier Laurent and Pedro M Machado are both corresponding authors.

Contributions:
Didier Laurent: Drafting/revision of the manuscript for content, including medical writing for content; Study concept or design; Analysis or intepretation of data
Jon Riek: Drafting/revision of the manuscript for content, including medical writing for content; Analysis or intepretation of data
Christopher DJ Sinclair: Drafting/revision of the manuscript for content, including medical writing for content; Major role in the acquisition of data
Parul Houston: Drafting/revision of the manuscript for content, including medical writing for content; Study concept or design; Analysis or intepretation of data
Ronenn Roubenoff: Drafting/revision of the manuscript for content, including medical writing for content; Analysis or intepretation of data
Dimitris A Papanicolaou: Drafting/revision of the manuscript for content, including medical writing for content; Analysis or intepretation of data
Attila Nagy: Drafting/revision of the manuscript for content, including medical writing for content; Analysis or intepretation of data
Steve Pieper: Drafting/revision of the manuscript for content, including medical writing for content; Analysis or intepretation of data
Tarek A Yousry: Drafting/revision of the manuscript for content, including medical writing for content; Analysis or intepretation of data
Michael G Hanna: Drafting/revision of the manuscript for content, including medical writing for content; Major role in the acquisition of data; Analysis or intepretation of data
John S Thornton: Drafting/revision of the manuscript for content, including medical writing for content; Study concept or design; Analysis or intepretation of data
Pedro M Machado: Drafting/revision of the manuscript for content, including medical writing for content; Major role in the acquisition of data; Study concept or design; Analysis or intepretation of data

Figure Count:
3

Table Count:
4

Search Terms:
[19] All Clinical trials, [54] Cohort studies, [58] Natural history studies (prognosis), [120] MRI, [185] Muscle disease

Acknowledgment:
PM Machado, JS Thornton, TA Yousry and MG Hanna are supported by the National Institute for Health Research (NIHR) University College London Hospitals (UCLH) Biomedical Research Centre (BRC). The views expressed are those of the authors and not necessarily those of the (UK) National Health Service (NHS), the NIHR, or the (UK) Department of Health. S Pieper is supported in part by the (US) National Institutes of Health (NIH) under grant P41EB015902.

Study Funding:
This study was funded by Novartis Pharmaceuticals.

Disclosures:
D Laurent, R Roubenoff and DA Papanicolaou are employees of Novartis and, as such, may be eligible for Novartis stock and stock options; J Riek is an employee of BioTel Research, which is an imaging CRO that was contracted by Novartis Pharma AG to perform the image analysis in this study; P Houston was also an employee of Novartis at the time of the study; A Nagy and S Pieper are employees of Isomics Inc, which is a technology development company that was contracted by Novartis Pharma AG to perform the semi-automatic image segmentation for individual muscle volume determination; A Nagy is also an employee of the University of Szeged, Szeged, Hungary; MG Hanna receives research funding from the Medical Research Council UK and has previously acted a a consultant for Novartis and for Orphazyme; PM Machado has received grants and/or honoraria from Abbvie, BMS, Celgene, Eli Lilly, Galapagos, Janssen, MSD, Novartis, Orphazyme, Pfizer, Roche and UCB Pharma. The other authors declare no relevant disclosures.

Preprint DOI:

Received Date:
2021-09-06

Accepted Date:
2022-04-11

Handling Editor Statement:
Solicited and externally peer reviewed. The handling editor was Anthony Amato, MD, FAAN.

ABSTRACT

Background and objectives: Limited data suggests that quantitative MRI (qMRI) measures have potential to be used as trial outcome measures in sporadic inclusion body myositis (sIBM), and as a non-invasive assessment tool to study sIBM muscle pathological processes. Our aim was to evaluate changes in muscle structure and composition using a comprehensive multi-parameter set of quantitative MRI (qMRI) measures and to assess construct validity and responsiveness of qMRI measures in people with sIBM.

Methods: Prospective observational cohort study with assessments at baseline (n=30) and 1-year (n=26). qMRI assessments: thigh muscle volume (TMV), inter/intramuscular adipose tissue (IMAT), muscle fat fraction (FF), muscle inflammation (T2 relaxation time), IMAT from T2* relaxation (T2*-IMAT), intermuscular connective tissue from T2* relaxation (T2*-IMCT), and muscle macromolecular structure from the magnetization transfer ratio (MTR). Physical performance assessments: sIBM Physical Functioning Assessment (sIFA), 6-minute walk distance, and quantitative muscle testing of the quadriceps. Correlations assessed using the Spearman correlation coefficient. Responsiveness assessed using the standardised response mean (SRM).

Results: After one year, we observed a reduction in TMV (6.8%, $p<0.001$) and muscle T2 (6.7%, $p=0.035$), an increase in IMAT (9.7%, $p<0.001$), FF (11.2%, $p=0.030$), connective tissue (22%, $p=0.995$) and T_2*-IMAT (24%, $p<0.001$), and alteration in muscle macromolecular structure (ΔMTR=-26%, $p=0.002$). Decrease in muscle T2 correlated with increase in T2*-IMAT ($r=-0.47$, $p=0.008$). Deposition of connective tissue and IMAT correlated with deterioration in sIFA ($r=0.38$,

p=0.032; r=0.34, p=0.048; respectively), while decrease in TMV correlated with decrease in QMT (r=0.36, p=0.035). The most responsive qMRI measures were T2*-IMAT (SRM=1.50), TMV (SRM=-1.23), IMAT (SRM=1.20), MTR (SRM=-0.83) and T2 relaxation time (SRM=-0.65).

Discussion: Progressive deterioration in muscle quality measured by qMRI is associated with decline in physical performance. Inflammation may play a role in triggering fat infiltration into muscle. qMRI provides valid and responsive measures that might prove valuable in sIBM experimental trials and assessment of muscle pathological processes.

Classification of evidence: This study provides Class I evidence that qMRI outcome measures are associated with physical performance measures in sIBM.

INTRODUCTION

Sporadic inclusion body myositis (sIBM) is a rare progressive and currently untreatable muscle disorder causing severe disability, yet recognized as the most common acquired muscle disease associated with aging.[1-4] While factors that trigger sIBM remain unknown, muscle biopsies of affected individuals show both inflammatory and degenerative changes.[5-9]

The etiopathogenesis of sIBM is controversial and probably multifactorial.[10-14] Whether the inflammatory changes observed in specific muscles precede myodegeneration[15] or are secondary to protein aggregation is still controversial. Treatments targeting the inflammatory component have not been successful in sIBM.[16, 17] For this reason, new efforts are now geared toward the development of muscle-regenerative drugs and drugs that target protein dyshomeostasis.[16-20]

Outcome assessment in sIBM has included measures of health-related quality of life, physical function, mobility, strength and endurance.[21, 22] While these assessments seek to provide a simple measurement of patients' functional status, the inherent variability in ambulatory outcomes can make these outcome measures relatively insensitive to small changes. It is also difficult to consider multiple muscle biopsies, either in time or in various parts of the body, to measure histopathological muscle changes, as these are invasive and resource-intensive procedures. Moreover, the disease is patchy, asymmetric and heterogeneous, and histopathological features can differ significantly within and between muscles in the same patient.

Magnetic resonance imaging (MRI) is diagnostically helpful in muscle disease and shows much promise as a tool to monitor disease progression and provide sensitive outcome measures for clinical trials.[23-25] As an alternative to serial muscle biopsies, MRI also appears

to be well suited for various biochemical measurements of skeletal muscle in direct line with the development of sIBM.[25] Thus, fat infiltration into the muscle can be measured by the Dixon method,[26] muscle oedema/inflammation can be assessed from fat-corrected muscle T2 maps,[27] macromolecular structure of the muscle cells by magnetization transfer[28] and muscle connective tissue from T2* values.[29] All these markers could potentially be used as responsive and objective endpoints of disease progression to test disease modifying effects of new drugs. These measurements may also clarify the role played by muscle oedema and the accumulation of fat and/or connective tissue in the progressive alteration of the patients' function. This knowledge could lead to a better choice of treatment candidates and options, with patients benefiting ultimately from a more personalized treatment approach for this complex disease.

Our aim was to evaluate changes in muscle structure and composition that occur in sIBM patients over one-year, using quantitative MRI (qMRI), and to assess the responsiveness and construct validity of qMRI measures.

MATERIALS AND METHODS

sIBM patients

A longitudinal, natural history cohort study was conducted on 184 patients between Feb-2015 and Jan-2017 in Canada, Sweden, UK, and USA.[30] Men and women aged ≥45 years, with an expert diagnosis of sIBM and fulfilling 2008 Hilton-Jones/MRC Centre for Neuromuscular Diseases,[31] 2011 European Neuromuscular Centre (ENMC),[32] or 2014 Lloyd/Greenberg criteria,[33] were recruited. More details on patient inclusion and exclusion criteria can be found in the **eMethods**.

The imaging sub-study was conducted at an add-on to the main study, at the single site in the UK, and all of the 30 patients consecutively recruited by this site participated in the sub-study, the results of which are shown here. Patients were excluded if they had concurrent diagnosis of any other disease that could interfere with outcome assessment of sIBM. In addition, muscle and fat volumes obtained by MRI from this group of patients were compared with those previously obtained from 47 healthy volunteers. The study was approved by the Research Ethics Committee and participants provided written informed consent. The MRI reader was blinded for clinical assessments, and clinical assessors were blinded for MRI readings. However, clinical evaluators and the MRI reader were not blinded for timepoints of assessment.

MRI acquisition, image analysis and outcome measures

All patients were scanned on a 1.5T clinical MR scanner (Avanto, Siemens Healthineers). Images of the thigh were acquired at baseline and one-year. Two-dimensional proton-density-weighted images (TR=4,840ms, TE=12ms, matrix=256x256, FOV=30cm, slice spacing=5mm) and volumetric interpolated breath-hold examination (VIBE) Dixon images (TR=24.6ms, TE=2.38ms, 4.76ms, matrix=256x192, FOV=30cm, slice spacing=5mm) of the thigh were acquired using the inherent body coil. A 3D SPGR (TR=65ms, TE=3ms, matrix=256x256, FOV=28cm, slice spacing=5mm) with and without magnetization transfer contrast (MTC), a seven-echo fat-saturated spin-echo sequence (TR=1500ms, TE=[15,30,45,60,75,90,105]ms, matrix=256x256, FOV=28cm, slice spacing=10mm) and a six-echo gradient echo sequence (TR=300ms, TE=[2.3,3.55,4.8,6.05,7.3,8.55]ms, matrix=256x256, FOV=28cm, slice spacing=10mm) were acquired at mid-thigh using a torso coil.

All images were analysed centrally by a single reader and reviewed by a single board certified radiologist from BioTel Research (Rochester, NY, US). The following qMRI outcome measures were assessed: thigh muscle volume (TMV), subcutaneous and inter/intramuscular adipose tissue (SCAT and IMAT) volumes, muscle fat fraction (FF), muscle inflammation (T2 relaxation time), IMAT from T2* relaxation (T2*-IMAT), intermuscular connective tissue from T2* relaxation (T2*-IMCT), and muscle macromolecular structure from the magnetization transfer ratio (MTR).[29, 34-36]

Thigh muscle volume (TMV), subcutaneous adipose tissue (SCAT) volume and inter/intramuscular adipose tissue (IMAT) volume were determined from the 2D proton-density-weighted images using the technique described by Positano et al.[35] Manual corrections were made to any inaccurate boundaries determined by the algorithm, as well as corrections to the labelling of muscle and fat tissue in the presence of artifacts. The muscle regions determined from the 2D proton-density-weighted images were then tracked to the Dixon images, and the average fat fraction (FF) in the muscle tissue was calculated for the whole thigh. The fat fraction at each voxel was calculated as $100f/(f+w)$, where f is the signal intensity in the fat image and w is the signal intensity in the water image.

A T_2 relaxation time map was calculated from the seven-echo fat-saturated spin-echo sequence assuming a mono-exponential decay.[36] Likewise, a T_2* relaxation time map was estimated using the six-echo gradient echo sequence assuming a mono-exponential decay. A magnetization transfer ratio (MTR) map was calculated using the 3D spoiled gradient echo (SPGR) sequence with and without magnetization transfer contrast (MTC) as $100(S_0-S_{MT})/S_0$,[34] where S_0 is the signal intensity in the SPGR image without MTC and S_{MT} is the signal intensity in the SPGR image with MTC. The reader then identified 11 different muscles at the mid-thigh on four slices, i.e. five muscles in the anterior (rectus femoris, vastus lateralis, vastus intermedius, vastus medialis, sartorius) and six muscles in the posterior

compartment (semitendinosus, semimembranosus, biceps femoris, gracilis, adductor magnus, adductor longus). The average T_2*, T_2, MTR and fat fraction were calculated for each of the identified muscles. T_2* voxel counts corresponding to intramuscular connective tissue (IMCT 4-8ms), IMAT (8-12ms) and muscle tissue (28-38ms) within the identified muscles were also determined.[29]

Csapo *et al.*[29] utilized a 3T magnet in their article, and used T2* relaxation times of 2-4ms for IMCT, 4-6ms for IMAT, and 14-19ms for muscle tissue. In this study, a 1.5T magnet was used. As local field variations due to tissue susceptibility variations are expected to be reduced by a factor of approximately 2 at 1.5T vs 3T, we assumed that T2* values would be increased by the same factor. Therefore, T2* thresholds retained were twice those presented by Csapo et al.[29]

As explained above, two different methods were used to determine the amount of IMAT in the muscles at mid-thigh. The first was based on the signal intensity in a proton-density-weighted image. Each muscle present in the image was outlined by a reader. The images were segmented into muscle, adipose tissue and background using a fuzzy c-means classification algorithm. The background voxels consisted of air, tendons, cortical bone, and any other tissue that appears dark in a typical proton-density-weighted image. The voxels labelled as adipose tissue within each muscle were classified as IMAT. In addition, the same muscles were outlined using the first echo of the multi-echo GRE sequence used to calculate the T2* map. For each muscle, the voxels that had a corresponding T2* value between 8 and 12ms were labelled as IMAT.

Individual thigh muscles were segmented from the 2D proton-density weighted MR images through the combined use of a signal thresholding and fuzzy pixel clustering approach as well as active contours. For muscle contours, the 3D Slicer semi-automated segmentation tool, an open source software platform (www.slicer.org), was utilized. The user selected seed

points on a subset of slices from the MR dataset, and then hermite spline interpolation technique was used for any slice that did not contain user-supplied seed points. The resulting segmented regions, which were then divided into individual lean muscle and IMAT volumes, were reviewed by the rater and, if necessary, corrected using manual editing tools. With this method, the reader identified 6 muscles in the anterior (rectus femoris [RF], vastus lateralis and intermedius [VLI], tensor fascia latae [TFL], sartorius [SAR], vastus medialis [VM]) and 5 muscles in the posterior compartment (semimembranosus [SM], gracilis [GRA], semitendinosus [ST], biceps femoris long head [BFL], biceps femoris short head [BFB]). Additional control points may have been added after visual inspection to incrementally refine the results of the segmentation.

sIBM Physical Functioning Assessment (sIFA)

Physical function was assessed using the sIFA.[37, 38] This disability questionnaire consists of 11 items scored on a 0 (no difficulty) to 10 (unable to do) numerical rating scale. These items describe general, upper and lower extremity, and swallowing functions. Total sIFA scores were transformed to a 0-100 scale, with higher scores reflecting greater disability.

Measures of muscle strength and mobility

Muscle strength was assessed using quantitative muscle testing (QMT) of the quadriceps muscle using the BTE™ Evaluator portable fixed dynamometer (BTE Technologies, Hanover, MD, USA). The maximum force generated by the subject from two post-warm-up trials was recorded for each muscle group.

Mobility was assessed using the 6-minute walking distance (6MWD), a widely used method to assess walking capability in neuromuscular diseases.[19, 39-42]

Data analysis and statistics

To correct for the amount of fatty infiltration into the thigh muscles, the relative thigh muscle volume was calculated as %TMV=100*TMV/(TMV+IMAT+SCAT). This value represents the percentage of voxels that have been labelled as muscle tissue throughout the thigh. Likewise, the relative IMAT is the percent of voxels in the same region that were labelled as IMAT. The sample size of the study was determined based on feasibility at the selected site. All values are expressed as means±standard error of the mean (SEM). Intergroup comparisons and time-course variations were analysed using a mixed effect model approach, with p-values adjusted for multiple testing using the Dunn–Šidák correction, and missing data treated as missing. Correlations were assessed using the Spearman correlation coefficient, and the magnitude of the observed correlation coefficient interpreted as proposed by Schober et al, without adjustment of p-values for multiple testing:[43] 0.00-0.10, negligible correlation; 0.10-0.39, weak correlation; 0.40-0.69, moderate correlation; 0.70-0.89, strong correlation; 0.90-1.00, very strong correlation. In order to describe the extent of variability for some of the parameters measured from study patients at baseline, coefficients of variation (CV) were also calculated as a percentage and defined as the ratio of the standard deviation of the mean. The standardised response mean (SRM) was used as a measure of responsiveness and it was calculated by dividing the mean change by the standard deviation of the change. Based on Cohen's thresholds, SRM values <0.5, ranging from 0.5 to 0.8, and >0.8 are deemed to indicate small, moderate and large responsiveness, respectively. Statistical analyses were done using GraphPad Prism software (version 8, GraphPad Software Inc., La Jolla, CA, USA), and a $p<0.05$ was considered statistically significant.

Data availability statement

Data are available upon reasonable request. Applications to access the data should be made to Novartis Pharmaceuticals.

Standard protocol approvals, registrations, and patient consents

The study protocol was approved by the South Central - Oxford B Research Ethics Committee (REC Reference 14/SC/1419). Informed consent was obtained from study participants.

RESULTS

Subject demographics

Baseline clinical and demographic data are summarized in Table 1. The study population had a mean age of 66 years, mean symptom/disease duration of 9 years, and was predominantly White (90%) and male (83%). Disability was clearly detected at the time of their enrolment marked by subnormal mean 6MWD (325±153 m) and QMT values (19.6±22.1 lbs or 8.9±10.0 Kg) and relatively high sIFA scores (47.6±23.8), but with large disparities within the whole group (i.e. CV values varying from 47% to 113% depending on the variable measured).

Baseline Assessments

The relative TMV at the start of the study ranged from 14.5% to 53.8%, with an average of 36.2%±12.4%, an indication of how significant but also variable muscle atrophy appeared to be in the enrolled group of sIBM patients as compared to normal healthy subjects (53.6%±11.1%, N=47, $p<0.001$ vs sIBM, Figure 1). Interestingly, while IMAT deposition is significantly increased in sIBM patients, the relative volume of SCAT remains similar to that of healthy subjects.

Figure 2 shows cross-sectional MR images of the thigh obtained from one patient at an early stage and another patient at a later stage of the disease. Along with different degrees of muscle atrophy, clear differences can also be observed between these two patients in terms of muscle oedema (T_2), marbling fat content (relative IMAT volume and T_2*-IMAT), muscle fat fraction (FF), presence of connective tissue and/or protein aggregate (T_2*-IMCT) and alteration in the macromolecular structure (MTR). These structural differences were accompanied by differences in functional status as marked by differences in both self-reported (sIFA) and objective measures (6MWD and QMT).

Baseline MRI characteristics (Table 1) measured at the group level (mean±SD [min-max]) showed a high degree of heterogeneity (i.e., with CV values ranging from 24% to 109%) for T_2: 37.7±8.9ms [27.3-73.5ms], relative IMAT volume: 40.2±15.6% [14.9-61.8%], T_2*-IMAT: 35.7±23.2% [2.8-82.7%], FF: 21.1±8.3% [9.5-41.7%], T_2*-IMCT: 0.88±0.96% [0.00-3.67%] and MTR values: 24.2±7.2 [9.0-36.8], reflecting a wide range of disease stages. Further analysis of the entire group also indicated greater presence of oedema (T_2: 43.5±11.3 *vs* 35.0±7.8ms, $p<0.001$) and specific alteration of the macromolecular structure (MTR: 20.7±7.3 *vs* 27.1±8.6, $p<0.001$) in anterior thigh muscles, when compared to posterior thigh muscles.

Finally, various significant moderate correlations (ranging from ±0.41 to ±0.68) were found between qMRI and functional variables measured at baseline (Table 2). In short, lower relative thigh muscle volume (%TMV) and higher relative muscle fat volume (i.e., both %IMAT and T2*-IMAT), the infiltration of lipids within muscle tissue (i.e., FF as a marker for the mixed pool of extra and intramyocellular lipids), as well as the accumulation of connective tissue and/or protein aggregate around the muscle (T_2*-IMCT) and the nature of muscle macromolecular structure (i.e., MTR) were associated with lower mobility and strength (6MWD and QMT) values and with impairment of physical function (higher sIFA

scores). However, the degree of muscular oedema (T2) was not significantly associated with the performance variables measured in the study. Notably, statistically significant weak to moderate correlations between qMRI outcome measures and disease duration (but not age) were observed at the cross-sectional level, further supporting the construct validity of qMRI assessments in a progressive muscle wasting disease like sIBM.

One-year assessments, responsiveness and correlations between change scores

Four out of 30 patients withdrew from the study, and, hence, did not undergo MRI assessment at the one-year follow-up. All patients who declined to participate in the 1-year visit did so because of time constraints and/or difficulties travelling to the site due to their disability. Significant changes were observed after 1-year for the majority of qMRI measures (Table 3), but not for physical performance tests, with the most responsive qMRI measures being T2*-IMAT (SRM=1.50), TMV (SRM=-1.23), IMAT (SRM=1.20), MTR (SRM=-0.83) and T2 relaxation time (SRM=-0.65).

Figure 3 depicts a loss in thigh muscle volume (TMV) of 174 ml (-6.8%, $p<0.001$), a concomitant gain in muscle fat (IMAT) of 169 ml (+9.7%, $p<0.001$), but no significant change in the subcutaneous adipose tissue volume (+47 ml or +1.6% SCAT, $p=0.999$). When broken down to individual muscles, muscle volume loss ranged from <1% (gracilis muscle) to -12.6% (vastus lateralis & intermedius [VLI] muscle), whereas IMAT showed increases ranging from +3.6% (tensor fascia latae [TFL] muscle) to +18.5% (biceps femoris [BFL] muscle). Interestingly, the IMAT deposition occurred more prominently ($p=0.02$) in posterior (+13.4%) than in anterior muscles (+8.5%).

Regarding other compositional features, as shown in eFigure 1, disease progression could also be characterized by an increase from 21.3% to 23.7% (+11.2%, $p=0.030$) in intra-muscular lipid content (FF) and further alteration in the muscle macromolecular structure, i.e., a decrease in MTR values from 20.7% to 15.3% (-26%, $p<0.001$) in anterior and from 27.1%

to 21.8% (-20%, p=0.010) in posterior muscles compartments. Furthermore, the decrease in muscle inflammation that was observed over the entire thigh after one-year (i.e., a -6.7% change in T2 relaxation rate from 38.9ms to 36.3ms, p=0.035) was found to be more significant in the posterior muscles (p=0.012) than in the anterior muscles (p=0.071). On the contrary, a trend for a larger increase in the T2*-IMCT %voxel was found in the anterior muscles (i.e., from 0.55% to 1.01% or +84%, p=0.077) vs. the posterior muscles (i.e., from 1.15% to 1.13% or -2.3%, p=0.503) of the thigh.

Correlation analysis between measurements made at baseline and changes after one-year showed that lower baseline T2 values were associated with higher deposition of marbling fat (ΔT2*-IMAT) after 1-year (r=0.49, p<0.001), more so in the anterior (r=0.56, p=0.002) than in the posterior (r=0.19, p=0.18) muscle compartments, possibly indicative of the progressive replacement of inflamed tissue by fat tissue (eFigure 2A). Similarly, to further support this concept, the change in T2*-IMAT was inversely correlated with the change in muscle T2, and this association was again stronger in the anterior than in the posterior muscle compartment (whole thigh muscle: r=-0.47, p=0.008; anterior muscle compartment: r=-0.62, p<0.001; posterior muscle compartment: r=-0.29, p=0.07) (eFigure 2A).

While small, but non-significant, changes in muscle performance (-4% in 6MWD, from 327±154 m to 314±149 m, p=0.981; -9.9% in QMT, from 19.6±21.7 lbs to 17.7±20.5 lbs, p=0.749) and physical function (+13.5% in sIFA score, from 52±26 to 59±25, p=0.287) were observed after one-year, only the decrease in TMV was weakly (albeit significantly) correlated with the decrease in QMT (r=0.36), while the increase in IMAT and the increase in the T2*-IMCT %voxel were both weakly correlated with the increase in sIFA (r=0.34 and r=0.38, respectively) (Table 4), highlighting the greater sensitivity of muscle qMRI over more conventional measures of physical performance. Finally, none of changes observed in the

MRI measurements were found to be significantly associated with neither the age of the patients nor the duration of their disease.

Classification of evidence

This study provides Class I evidence that qMRI outcome measures are associated with physical performance measures in sIBM.

DISCUSSION

This study shows that along with loss of muscle mass, there is progressive deterioration in muscle quality in sIBM that was associated with a functional decline. qMRI measures changed significantly during the 1-year follow-up period and several measures were shown to be highly responsive, namely inter/intramuscular fat deposition, thigh muscle volume and muscle macromolecular structure. Deposition of connective and inter/intramuscular adipose tissue correlated with deterioration in physical function, and higher baseline muscle inflammation and decrease in muscle inflammation correlated with an increase in inter/intramuscular adipose tissue deposition after 1-year, suggesting that muscle water changes (inflammation) may play a role in triggering fat infiltration into muscle, a typical characteristic of sIBM muscle tissue. Finally, at baseline, multiple qMRI measures correlated with measures of physical function, mobility and strength. Therefore, qMRI outcome measures are valid and responsive, and might prove valuable in sIBM experimental trials and assessment of muscle pathological processes.

For effective monitoring of investigational drug treatments in diseases where muscle atrophy occurs heterogeneously, this study also highlights the importance of assessing

quantitative and qualitative changes at the individual muscle level. High spatial resolution and unparalleled soft tissue contrast make qMRI the ideal tool to measure muscle volume with high precision. However, manual segmentation of individual muscles from MR image series can be challenging and time consuming. The main difficulty resides in the correct delineation of muscle boundaries with respect to SCAT and IMAT (or "marbled" fat), which is defined as the visible adipose tissue beneath the muscle fascia, between muscles, and even within the muscle, but outside the actual muscle cell.

Decreased muscle performance and physical function have both been associated with high levels of IMAT.[44] Here we show results obtained from the freely downloadable 3D Slicer algorithm[45] that was developed for semi-automated segmentation of individual thigh muscles. In sIBM, individual muscles were very heterogeneous, both in terms of muscle atrophy and fatty infiltration. Whether such differences result from distinct physiological and biochemical properties between all these muscles before the disease is diagnosed remains to be determined. In spite of this, such characterization may prove particularly useful when assessing the effects of new muscle therapies on the restoration of muscle structure and function, and may help to examine more precisely the relative contribution of each muscle to the overall function of these patients.

Especially in patients at a relatively early stage of the disease, fat-saturated T_2 images showed increased signal in patchy areas of thigh muscle suggesting presence of oedema, an accompanying sign of inflammation in sIBM patients, also demonstrated by muscle biopsies.[5] Notably, this inflammation did not appear to expand significantly during the one-year observation period. If anything, it rather seemed to disappear/reduce in favour of a progressive deposition of fatty tissue both in the anterior and posterior thigh muscles, as supported by the inverse correlation observed between T_2 and T_2*-IMAT values. This new finding could strengthen the aetiopathogenic role of muscle inflammation in sIBM, as already

suggested by Benveniste *et al.*[15] However, only a thorough analysis of the images seeking to demonstrate the co-location between the disappearance of the oedema and the appearance of the fatty tissue would bring more definitive evidence of this mechanism. Many studies conducted so far have pointed out that immunomodulatory or immunosuppressive treatments are not effective or only transiently effective in sIBM. Perhaps these treatments would have been more effective if they had been tested only in patients with high T2 values. It is interesting to note that the decrease in physical performance in sIBM does not seem to be associated with the emergence of tissue inflammation, with functional impact being mainly determined by degenerative features such as fat, fibrosis and abnormal protein aggregation.[8, 9, 46] Whether the observed increase in T2*-IMCT in our study reflects the continuous accumulation of protein aggregates in skeletal muscle remains to be explored.

In a small Phase 2A sIBM study, treatment with bimagrumab,[47] a fully human monoclonal antibody that binds to the activin type II receptor (ActRII), resulted in a muscle anabolic response (ie, higher TMV and lean body mass) that seemed to translate into a functional improvement (ie, higher 6MWD). This potential beneficial effect of ActRII inhibition could not be confirmed in the large RESILIENT trial, in which the primary objective of improving the 6MWD was not reached, despite a modest dose-dependent increase in lean body mass noted with bimagrumab.[19, 20] This could perhaps illustrate the need for a greater skeletal muscle volume response to such anabolic treatment and/or additional patient interventions (e.g., co-medication and/or physiotherapy) for substantial improvement in the clinical condition to occur. Furthermore, skeletal muscle volume alone does not necessarily reflect the quality and functionality of the muscle tissue. The multi-parameter qMRI approach that we propose and validate in the current study has therefore potential for application in clinical trials. It provides more granular and comprehensive information about muscle structure/morphology/composition (beyond muscle volume) that

could help to better interpret trial results, especially when there is an apparent discrepancy between the measured anabolic response and clinical outcomes. Furthermore, establishing a stronger relationship between muscle structure and muscle function in sIBM patients could also benefit from the use of more precise functional tests, and the utility of muscle MRI could then be more clearly revealed. Existing functional/mobility endpoints based on patient self-reporting and one-off assessments lack sensitivity. In contrast, wearable digital technology may offer more real-world solutions and the resulting mobility and activity-based outcomes could potentially better describe the patients' condition. Additional studies will be necessary to elucidate these points.

Irrespective of these considerations, our data would support the use of thigh muscle volume (TMV), fat volume (IMAT or T2%-IMAT), MTR and muscle inflammation (T2 relaxation time), with absolute group mean SRM values ranging from 0.65 to 1.50, as the most responsive measures for a primary endpoint in clinical trials, allowing a significant reduction in sample size, as outlined by Lehr et al.[48] T2 relaxation time would be the endpoint of choice for studies focusing on muscle inflammation, while structural endpoints such as TMV and IMAT volume appear as obvious endpoint solutions for studies focusing on muscle wasting/atrophy. MTR may also be of particular interest because of the information it provides on muscle composition. Muscle atrophy is accompanied by a decline in the complexity of the macromolecular structure, as reflected by lower MTR values,[28, 49, 50] which could theoretically result in impaired muscle contractility, and ultimately the patient's function. In this context, MTR could then be used as an early and surrogate marker of muscle function. Additional studies with longer follow-up periods, and potentially more comprehensive functional measures (including global measures of physical activity) will help further substantiate these considerations.

This study had several limitations. Firstly, the sample size is relatively small, and it is therefore difficult to show strong correlations between each of the variables measured independently. However, this study was carried out at a single site, which made it possible to minimize part of the variability inherent to the imaging technique used (e.g., single scanner, operator-dependent tests, etc.). Conversely, the extent to which the MRI measurements presented here can be performed with the same level of accuracy and reliability in multi-site studies will require further investigation. Secondly, some of the imaging parameters (i.e., T2*-IMCT and muscle MTR) are measures that, to our best knowledge, have been applied for the first time in sIBM patients. It is therefore important that they are the subject of additional investigations and validation by parallel histological data to be able to strengthen interpretation. Third, this is a 1-year study, and examining changes over longer periods of time would have been informative in terms of better understanding disease dynamics and medium- to long-term rates of disease progression and corresponding MRI changes. Finally, physical performance measures, such as 6MWD, may be subject to variation due to factors other than muscle weakness, thus limiting the interpretation of changes as measures of disease progression, particularly in patients whose lower extremity disease progresses slowly during an observation period of only one-year. To what extent more continuous monitoring of gait characteristics by the use of digital technologies could compensate for this lack of sensitivity would also be worthy of further exploration in future trials.

In summary, this study showed that qMRI outcome measures are valid and allow monitoring of muscle morphometry and composition over time with high responsiveness, particularly loss of thigh muscle volume (muscle wasting) and accumulation of inter/intramuscular adipose tissue (fat deposition). This study also showed that the increase in marbling fat is inversely correlated with a decrease in muscle oedema, suggesting that inflammation may play a role in triggering fatty infiltration of muscle tissue. Multi-parameter

qMRI assessments could potentially shed more light on disease pathological processes and mechanism of action of experimental drugs.

WNL-2022-200760_sup -- http://links.lww.com/WNL/C114

REFERENCES

1. Greenberg SA. Inclusion body myositis: clinical features and pathogenesis. Nat Rev Rheumatol 2019;15:257-272.
2. Jabari D, Vedanarayanan VV, Barohn RJ, Dimachkie MM. Update on Inclusion Body Myositis. Curr Rheumatol Rep 2018;20:52.
3. Machado PM, Ahmed M, Brady S, et al. Ongoing developments in sporadic inclusion body myositis. Curr Rheumatol Rep 2014;16:477.
4. Schmidt J, Dalakas MC. Inclusion body myositis: from immunopathology and degenerative mechanisms to treatment perspectives. Expert Rev Clin Immunol 2013;9:1125-1133.
5. Arahata K, Engel AG. Monoclonal antibody analysis of mononuclear cells in myopathies. III: Immunoelectron microscopy aspects of cell-mediated muscle fiber injury. Ann Neurol 1986;19:112-125.
6. Dalakas MC. Polymyositis, dermatomyositis and inclusion-body myositis. N Engl J Med 1991;325:1487-1498.
7. Engel AG, Arahata K. Monoclonal antibody analysis of mononuclear cells in myopathies. II: Phenotypes of autoinvasive cells in polymyositis and inclusion body myositis. Ann Neurol 1984;16:209-215.
8. Oldfors A, Moslemi AR, Fyhr IM, Holme E, Larsson NG, Lindberg C. Mitochondrial DNA deletions in muscle fibers in inclusion body myositis. J Neuropathol Exp Neurol 1995;54:581-587.
9. Temiz P, Weihl CC, Pestronk A. Inflammatory myopathies with mitochondrial pathology and protein aggregates. J Neurol Sci 2009;278:25-29.
10. Askanas V, Engel WK. Inclusion-body myositis, a multifactorial muscle disease associated with aging: current concepts of pathogenesis. Curr Opin Rheumatol 2007;19:550-559.
11. Dalakas MC. Mechanisms of disease: signaling pathways and immunobiology of inflammatory myopathies. Nat Clin Pract Rheumatol 2006;2:219-227.
12. Dalakas MC. Sporadic inclusion body myositis--diagnosis, pathogenesis and therapeutic strategies. Nat Clin Pract Neurol 2006;2:437-447.

13. Machado P, Brady S, Hanna MG. Update in inclusion body myositis. Curr Opin Rheumatol 2013;25:763-771.

14. Nagaraju K, Casciola-Rosen L, Lundberg I, et al. Activation of the endoplasmic reticulum stress response in autoimmune myositis: potential role in muscle fiber damage and dysfunction. Arthritis Rheum 2005;52:1824-1835.

15. Benveniste O, Stenzel W, Hilton-Jones D, Sandri M, Boyer O, van Engelen BG. Amyloid deposits and inflammatory infiltrates in sporadic inclusion body myositis: the inflammatory egg comes before the degenerative chicken. Acta Neuropathol 2015;129:611-624.

16. Rose MR, Jones K, Leong K, et al. Treatment for inclusion body myositis. Cochrane Database of Systematic Reviews 2015.

17. Solorzano GE, Phillips LH, 2nd. Inclusion body myositis: diagnosis, pathogenesis, and treatment options. Rheum Dis Clin North Am 2011;37:173-183, v.

18. Ahmed M, Machado PM, Miller A, et al. Targeting protein homeostasis in sporadic inclusion body myositis. Sci Transl Med 2016;8:331ra341.

19. Hanna MG, Badrising UA, Benveniste O, et al. Safety and efficacy of intravenous bimagrumab in inclusion body myositis (RESILIENT): a randomised, double-blind, placebo-controlled phase 2b trial. Lancet Neurol 2019;18:834-844.

20. Amato AA, Hanna MG, Machado PM, et al. Efficacy and Safety of Bimagrumab in Sporadic Inclusion Body Myositis: Long-term Extension of RESILIENT. Neurology 2021;96:e1595-e1607.

21. Rider LG, Aggarwal R, Machado PM, et al. Update on outcome assessment in myositis. Nat Rev Rheumatol 2018;14:303-318.

22. Sangha G, Yao B, Lunn D, et al. Longitudinal observational study investigating outcome measures for clinical trials in inclusion body myositis. J Neurol Neurosurg Psychiatry 2021.

23. Dion E, Cherin P, Payan C, et al. Magnetic resonance imaging criteria for distinguishing between inclusion body myositis and polymyositis. J Rheumatol 2002;29:1897-1906.

24. Kubinova K, Dejthevaporn R, Mann H, Machado PM, Vencovsky J. The role of imaging in evaluating patients with idiopathic inflammatory myopathies. Clin Exp Rheumatol 2018;36 Suppl 114:74-81.

25. Morrow JM, Sinclair CD, Fischmann A, et al. MRI biomarker assessment of neuromuscular disease progression: a prospective observational cohort study. Lancet Neurol 2016;15:65-77.

26. Wren TA, Bluml S, Tseng-Ong L, Gilsanz V. Three-point technique of fat quantification of muscle tissue as a marker of disease progression in Duchenne muscular dystrophy: preliminary study. AJR Am J Roentgenol 2008;190:W8-12.

27. Yao L, Gai N. Fat-corrected T2 measurement as a marker of active muscle disease in inflammatory myopathy. AJR Am J Roentgenol 2012;198:W475-481.

28. Sinclair CD, Morrow JM, Miranda MA, et al. Skeletal muscle MRI magnetisation transfer ratio reflects clinical severity in peripheral neuropathies. J Neurol Neurosurg Psychiatry 2012;83:29-32.

29. Csapo R, Malis V, Sinha U, Du J, Sinha S. Age-associated differences in triceps surae muscle composition and strength - an MRI-based cross-sectional comparison of contractile, adipose and connective tissue. BMC Musculoskelet Disord 2014;15:209.

30. Goyal N, Houston P, Machado P, et al. A Prospective Natural History Study of Sporadic Inclusion Body Myositis: 1-Year Results (P1.134). Neurology 2017;88.

31. Hilton-Jones D, Miller A, Parton M, Holton J, Sewry C, Hanna MG. Inclusion body myositis: MRC Centre for Neuromuscular Diseases, IBM workshop, London, 13 June 2008. Neuromuscul Disord 2010;20:142-147.

32. Rose MR, Group EIW. 188th ENMC International Workshop: Inclusion Body Myositis, 2-4 December 2011, Naarden, The Netherlands. Neuromuscul Disord 2013;23:1044-1055.

33. Lloyd TE, Mammen AL, Amato AA, Weiss MD, Needham M, Greenberg SA. Evaluation and construction of diagnostic criteria for inclusion body myositis. Neurology 2014;83:426-433.

34. Henkelman RM, Stanisz GJ, Graham SJ. Magnetization transfer in MRI: a review. NMR Biomed 2001;14:57-64.

35. Positano V, Christiansen T, Santarelli MF, Ringgaard S, Landini L, Gastaldelli A. Accurate segmentation of subcutaneous and intermuscular adipose tissue from MR images of the thigh. J Magn Reson Imaging 2009;29:677-684.

36. Raya JG, Dietrich O, Horng A, Weber J, Reiser MF, Glaser C. T2 measurement in articular cartilage: impact of the fitting method on accuracy and precision at low SNR. Magn Reson Med 2010;63:181-193.

37. Williams V, Coles T, Gnanasakthy A, et al. Psychometric validation of a patient-reported measure of physical functioning in sporadic inclusion body myositis. Muscle Nerve 2016;54:658-665.
38. DeMuro C, Lewis S, Lowes L, Alfano L, Tseng B, Gnanasakthy A. Development of the sporadic inclusion body myositis physical functioning assessment. Muscle Nerve 2016;54:653-657.
39. Kierkegaard M, Tollback A. Reliability and feasibility of the six minute walk test in subjects with myotonic dystrophy. Neuromuscul Disord 2007;17:943-949.
40. McDonald CM, Henricson EK, Han JJ, et al. The 6-minute walk test as a new outcome measure in Duchenne muscular dystrophy. Muscle Nerve 2010;41:500-510.
41. Montes J, McDermott MP, Martens WB, et al. Six-Minute Walk Test demonstrates motor fatigue in spinal muscular atrophy. Neurology 2010;74:833-838.
42. Hogrel JY, Allenbach Y, Canal A, et al. Four-year longitudinal study of clinical and functional endpoints in sporadic inclusion body myositis: implications for therapeutic trials. Neuromuscul Disord 2014;24:604-610.
43. Schober P, Boer C, Schwarte LA. Correlation Coefficients: Appropriate Use and Interpretation. Anesth Analg 2018;126:1763-1768.
44. Hilton TN, Tuttle LJ, Bohnert KL, Mueller MJ, Sinacore DR. Excessive adipose tissue infiltration in skeletal muscle in individuals with obesity, diabetes mellitus, and peripheral neuropathy: association with performance and function. Phys Ther 2008;88:1336-1344.
45. Kapur T, Pieper S, Fedorov A, et al. Increasing the impact of medical image computing using community-based open-access hackathons: The NA-MIC and 3D Slicer experience. Med Image Anal 2016;33:176-180.
46. Engel WK. The essentiality of histo- and cytochemical studies of skeletal muscle in the investigation of neuromuscular disease. 1962. Neurology 1998;51:655 and 617 pages following.
47. Amato AA, Sivakumar K, Goyal N, et al. Treatment of sporadic inclusion body myositis with bimagrumab. Neurology 2014;83:2239-2246.
48. Lehr R. Sixteen S-squared over D-squared: a relation for crude sample size estimates. Stat Med 1992;11:1099-1102.
49. Schwenzer NF, Martirosian P, Machann J, et al. Aging effects on human calf muscle properties assessed by MRI at 3 Tesla. J Magn Reson Imaging 2009;29:1346-1354.
50. Vital A, Vital C, Rigal B, Decamps A, Emeriau JP, Galley P. Morphological study of the aging human peripheral nerve. Clin Neuropathol 1990;9:10-15.

Table 1. Baseline clinical and demographic characteristics of the study population (N=30).

Age, years, mean (SD)	65.6 (10.1)
Sex, male, n (%)	25 (83.3)
Ethnicity, n (%):	
White	27 (90)
Asian	2 (6.7)
Black	1 (3.3)
Disease duration (years)	8.9 (4.07)
Use of walking aids, n (%):	
Inside or around the home	12 (40)
Outside the home	18 (60)
Patients with dysphagia, n (%)	16 (53.3)
sIFA in arbitrary units, mean (SD)	47.6 (23.8)
6MWD in meters, mean (SD)	325 (153)
QMT (quadriceps), mean (SD):	
in lbs	19.6 (22.1)
in Kg	8.9 (10)
Whole-thigh MRI outcome measures, means (SD) (CV):	
Thigh muscle volume (TMV) in ml	2563 (877) (34%)
Relative TMV in %	36.2 (12.4) (34%)
Intra/inter-muscle adipose tissue (IMAT) volume in ml	1745 (877) (50%)
Relative IMAT volume in %	40.2 (15.6) (39%)
Sub-cutaneous adipose tissue (SCAT) volume in ml	2919 (1011) (35%)
Relative IMAT volume in %	39.2 (9.9) (25%)

Muscle fat fraction (FF) in %	21.1 (8.33) (39%)
Muscle magnetization transfer ratio (MTR) in %	24.2 (7.2) (30%)
Muscle T_2 relaxation rate in ms	37.7 (8.9) (24%)
Muscle T_2* relaxation rate in ms	21.3 (6.1) (29%)
% of T_2*-IMCT voxels	0.88 (0.96) (109%)
% of T_2*-IMAT voxels	35.7 (23.23) (65%)
% of T_2*-Muscle voxels	60.4 (22.26) (37%)

sIFA: sIBM physical functioning assessment, QMT: quantitative muscle testing, 6MWD: 6-minute walk distance, TMV: thigh muscle volume, IMAT: inter/intra muscle adipose tissue, FF: fat fraction, IMCT: intramuscular connective tissue, MTR: magnetization transfer ratio.

Table 2. Correlations of multi-parametric MRI findings with age, disease duration and observed functional, mobility and strength outcomes in sIBM patients at baseline (N=30).

		Thigh muscle characteristics						
		%TMV (ml)	**%IMAT (ml)**	**T_2 (ml)**	**FF (%)**	**T_2*-IMCT (%voxels)**	**T2*-IMAT (%voxels)**	**MTR (%)**
Patient characteristics and physical performance tests	**Age (years)**	-0.01 (p=0.476)	0.14 (p=0.231)	0.05 (p=0.400)	0.07 (p=0.355)	-0.12 (p=0.271)	-0.09 (p=0.318)	0.08 (p=0.331)
	DD (years)	-0.52* (p=0.002)	0.64* (p<0.001)	-0.31* (p=0.048)	0.47* (p=0.004)	0.37* (p=0.022)	0.52* (p=0.002)	-0.44* (p=0.007)
	sIFA (score)	-0.32 (p=0.088)	0.19 (p=0.319)	0.25 (p=0.174)	0.53* (p=0.002)	0.25 (p=0.185)	0.33 (p=0.079)	-0.27 (p=0.144)
	6MWD (m)	0.52* (p=0.003)	-0.54* (p=0.003)	0.23 (p=0.230)	-0.66* (p<0.001)	-0.36 (p=0.054)	-0.52* (p=0.004)	0.34 (p=0.068)
	QMT (lbs)	0.65* (p<0.001)	-0.41* (p=0.025)	0.12 (p=0.546)	-0.68* (p<0.001)	-0.53* (p=0.003)	-0.57* (p=0.001)	0.43* (p=0.019)

Spearman correlation coefficients are shown for each pair of variables along with their respective p value. Significant correlations are highlighted with an asterisk (*). DD: disease duration, sIFA: sIBM physical functioning assessment, 6MWD: 6-minute walk distance, QMT: quantitative muscle testing, %TMV: relative thigh muscle volume, %IMAT: relative inter/intra-muscle adipose tissue volume, T_2: spin-spin relaxation rate, FF: fat fraction, IMCT: intramuscular connective tissue, MTR: magnetization transfer ratio.

Table 3. Changes measured after a one-year follow-up in MRI-derived thigh muscle characteristics and functional, mobility and strength related outcomes in sIBM patients (N=26).

	Mean (SD)	Adjusted p-value	SRM
Whole-thigh MRI characteristics:			
ΔTMV (ml)	-174 (142)	<0.001*	-1.23
ΔIMAT (ml)	+169 (141)	<0.001*	1.20
ΔSCAT (ml)	+47 (340)	0.999	0.14
ΔT2 (ms)	-2.59 (3.95)	0.035*	-0.65
ΔFF (%)	+2.39 (5.57)	0.030*	0.43
ΔT2*-IMCT (% of voxels)	+0.20 (1.17)	0.995	0.17
ΔT2*-IMAT (% of voxels)	+8.56 (5.70)	<0.001*	1.50
ΔMTR (%)	-5.35 (6.47)	0.002*	-0.83
Physical performance tests			
ΔsIFA (score)	+6.50 (14.9)	0.287	0.44
Δ6MWD (m)	-13.0 (62.9)	0.981	-0.21
ΔQMT (lbs)	-1.94 (6.8)	0.749	-0.29

Changes from baseline are denoted from the use of Δ in the variable name. Significant changes are highlighted with an asterisk (*). SRM values may be interpreted based on Cohen's thresholds (>0.8 large; 0.5 to 0.8 moderate, and <0.5 small). SRM: standardized response mean, %TMV: relative thigh muscle volume, %IMAT: relative inter/intra-muscle adipose tissue volume, %SCAT: relative subcutaneous adipose tissue volume, T_2: spin-spin relaxation rate, FF: fat fraction, IMCT: intramuscular connective tissue , MTR: magnetization transfer ratio, sIFA: sIBM physical functioning assessment, 6MWD: 6-minute walk distance, QMT: quantitative muscle testing.

Table 4. Correlations between the changes measured after a one-year follow-up in MRI-derived thigh muscle characteristics and functional, mobility and strength related outcomes in sIBM patients (N=26).

		Thigh muscle characteristics						
		ΔTMV (ml)	**ΔIMAT (ml)**	**ΔT_2 (ms)**	**ΔFF (%)**	**ΔT_2*-IMCT (%voxels)**	**ΔT2*-IMAT (%voxels)**	**ΔMTR (%)**
Physical performance tests	**ΔsIFA (score)**	0.097 (p=0.322)	0.340* (p=0.048)	0.269 (p=0.097)	-0.165 (p=0.216)	0.376* (p=0.032)	-0.025 (p=0.452)	-0.279 (p=0.088)
	Δ6MWD (m)	-0.285 (p=0.088)	0.127 (p=0.278)	0.197 (p=0.177)	-0.081 (p=0.353)	-0.108 (p=0.308)	-0.062 (p=0.386)	-0.098 (p=0.325)
	ΔQMT (lbs)	0.362* (p=0.035)	0.142 (p=0.245)	0.236 (p=0.123)	-0.255 (p=0.105)	0.268 (p=0.093)	-0.196 (p=0.169)	0.236 (p=0.123)
Patient characteristics	**Age (years)**	-0.159 (p=0.218)	-0.186 (p=0.181)	0.091 (p=0.328)	-0.095 (p=0.322)	-0.066 (p=0.375)	-0.278 (p=0.084)	0.323 (p=0.054)
	Disease duration	-0.205 (p=0.157)	-0.033 (p=0.437)	-0.282 (p=0.081)	-0.003 (p=0.495)	-0.162 (p=0.214)	-0.057 (p=0.391)	-0.047 (p=0.409)

	(years)							

Changes from baseline are denoted from the use of Δ in the variable name. Spearman correlation coefficients are shown for each pair of variables along with their respective p value. Significant correlations are highlighted with an asterisk (*). sIFA: sIBM physical functioning assessment, 6MWD: 6-minute walk distance, QMT: quantitative muscle testing, TMV: thigh muscle volume, IMAT:inter/intra-muscle adipose tissue volume, T_2: spin-spin relaxation rate, FF: fat fraction, IMCT: intramuscular connective tissue, MTR: magnetization transfer ratio.

Figure 1. Comparison of muscle and fat volumes between healthy subjects and sIBM patients.

TMV: thigh muscle volume, IMAT: inter/intra muscle adipose tissue, SCAT: subcutaneous adipose tissue. ***p<0.0001, sIBM patients vs healthy controls.

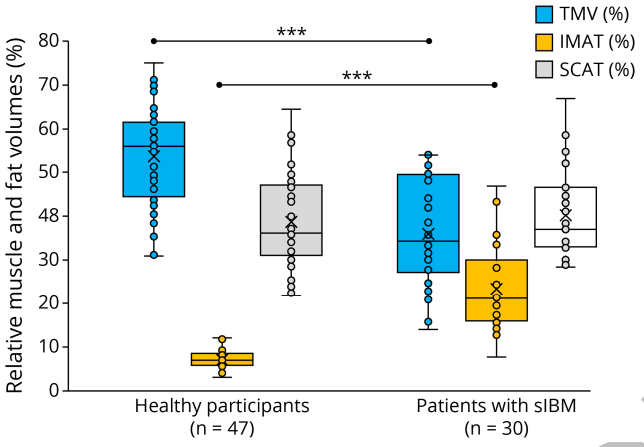

Figure 2. Thigh muscle structure and composition in sIBM patients.

Illustration of multi-parametric MRI recordings at baseline in two different sIBM patients. The first patient (A) is at an early stage of the disease (ie, sIFA 16, 6MWD 462 m, QMT 39.2 lbs) and the second patient (B) is at a more advanced stage of the disease (i.e. sIFA 75, 6MWD 90 m, QMT 9.0 lbs). sIFA: sIBM physical functioning assessment, QMT: quantitative muscle testing, 6MWD: 6-minute walk distance, TMV: thigh muscle volume, IMAT: inter/intra muscle adipose tissue, FF: fat fraction, IMCT: intramuscular connective tissue, MTR: magnetization transfer ratio.

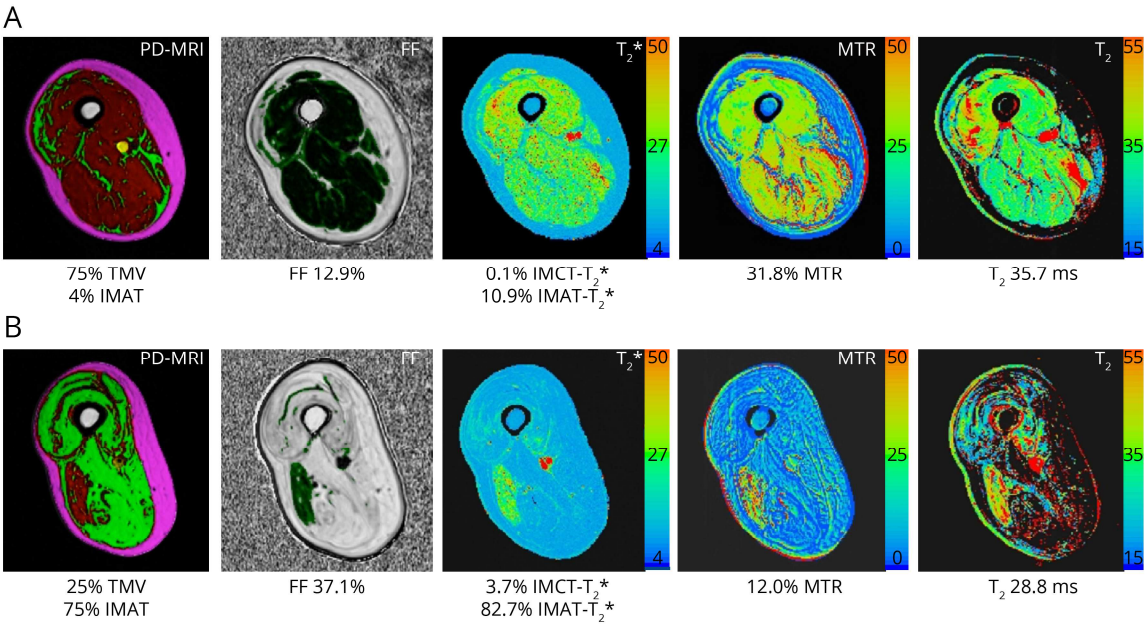

Figure 3. sIBM disease progression related to muscle structure.

Changes observed in sIBM patients after a one-year follow-up in A) thigh muscle volume (TMV) and associated intra/inter-muscle adipose tissue (IMAT) and sub-cutaneous adipose (SCAT) volumes, as well as changes in B) individual thigh muscle and associated IMAT volumes as measured by using the 3D-slicer segmentation approach. A segmentation example of anterior thigh muscles and the corresponding 3D-reconstruction is shown in the center. TMV: thigh muscle volume, IMAT: inter/intra muscle adipose tissue, SCAT: subcutaneous adipose tissue, RF: rectus femoris, VLI: vastus lateralis & intermedius, TFL: tensor fascia latae, SAR: sartorius, VM: vastus medialis, SM: semimenbranosus, GRA: gracilis, ST: semitendinosus, BFL: biceps femoris long head, BFB: biceps femoris short head. Values are means±SE, *Adjusted p<0.05, **Adjusted p<0.001, ***Adjusted p<0.0001, one-year vs Baseline (Bsl).